

Formability Modeling with LS-DYNA

Torodd Berstad, Odd-Geir Lademo, Ketill O. Pedersen

SINTEF Materials and Chemistry, NO-7465 Trondheim, Norway

Odd S. Hopperstad

Department of Structural Engineering, Norwegian University of Science and Technology,

NO-7491 Trondheim, Norway

Abstract

This paper presents how the process of loss of stability, as described by the classical theory of Marciniak and Kuczynski, can be represented in non-linear finite element analyses with LS-DYNA. As will be seen, this is strongly dependent upon proper constitutive equations and parameters for the sheet material at hand. Of this reason two user-defined sub-routines for weakly and strongly textured aluminum alloys, respectively, have been implemented. Further, a non-local instability criterion has been implemented in order to detect incipient plastic instability. Next, some inhomogeneity must be introduced in the finite element model. In further analogy to the work of Marciniak and Kuczynski the inhomogeneity can be introduced either to the material properties or to the thickness. In order to perform the calculations in an efficient way, an automated procedure – called an FLD-calculator – has been created. Finally, the FEM-based calculations are compared with analytical and experimental results.

Introduction

In a variety of applications there is a demand for optimized components made out of sheet materials or thin-walled extrusions, often requiring exploitation of the material to the verge of strain localization and material failure. Presently, and in the future, this calls upon skill-full use of non-linear finite element programs where the mentioned phenomena should be represented. Especially, robust design and production of light but crashworthy structural components in aluminum for the automotive industry are challenging tasks, involving development of alloys and manufacturing processes, structural design and crashworthiness analysis. Both recrystallized and non-recrystallized extruded aluminum alloys have typically strong crystallographic textures that lead to anisotropy in strength, plastic flow and ductility.

Based upon the classical instability analysis of Marciniak and Kuczynski [1], Barlat [2] argue that accurate prediction of localized necking for biaxial (stretch-stretch) deformation states is very sensitive to the shape of the yield surface. Here, two yield criteria for metals with orthotropic anisotropy proposed by Barlat and Lian [3] and Barlat et al. [4] have been adopted in the constitutive models applied to formability analysis. The former yield criterion is adopted for alloys with weak texture, while the latter accounts for strong texture. The main ingredients of the elastoplastic constitutive models are the anisotropic yield criterion, associated flow rule, a non-linear isotropic hardening rule and ductile fracture criteria (critical-thickness-strain and Cockcroft-Latham [5] criteria). The two constitutive models for weakly and strongly textured materials have been implemented in LS-DYNA [6] as user-subroutines.

Searching further inspiration from the classical instability analysis of Marciniak and Kuczynski, it is realized that – in ideal loading cases – inhomogeneity must be introduced in the finite element model. Here, it has been chosen to represent the inhomogeneity by a Gauss distributed stochastic variable. At present, either thickness or yield stress inhomogeneity can be represented. Further, to detect incipient plastic instability a non-local instability criterion has been implemented in LS-DYNA. In addition, a numerical tool for calculation of forming limit diagrams, called an FLD calculator, has been developed for use with LS-DYNA.

Formability Modeling

In their original paper, Marciniak and Kuczynski [1] assume that an initial heterogeneity in the thickness of the material is present, and they assess the plastic instability phenomenon using the two-zone model shown in Figure 1. The heterogeneity is described in terms of a groove (b) inclined at an angle ω to the minor principal stress direction. The thickness inside the groove is t_b while the thickness outside is t_a . The initial equivalent inhomogeneity factor is defined as the ratio

$$f_0 = \left(\frac{t_b}{t_a} \right)_0 \quad (1)$$

A biaxial stress state is imposed on the homogeneous region (a) with a constant ratio of strains, $\rho_a = \Delta\varepsilon_{a2} / \Delta\varepsilon_{a1}$, and the evolution of the strain rates in both regions (a) and (b) are examined. The plastic strain increment in the thickness direction has to be larger inside the groove than outside, $\Delta\varepsilon_{b3} > \Delta\varepsilon_{a3}$, to satisfy force equilibrium across the groove. Hence, the groove will grow in a certain manner depending on among other factors the magnitude of the initial heterogeneity. The limiting strains are achieved when the ratio $\beta = \Delta\varepsilon_{b3} / \Delta\varepsilon_{a3}$ approaches a critical value β_{cr} corresponding to local instability, i.e. a non-local instability criterion that reads

$$\beta = \Delta\varepsilon_{b3} / \Delta\varepsilon_{a3} = \beta_{cr} \quad (2)$$

For a given strain path, the forming limit is obtained for the groove orientation ω that leads to the minimum calculated limiting strains. For a material exhibiting planar isotropy and subject to a linear strain path, the critical groove orientation corresponds to an angle $\omega = 0^\circ$ in the whole stretching range (Barata da Rocha et al. [7]).

The original assumptions for the Marciniak-Kuczynski analysis were planar isotropy, Hill's yield criterion (Hill [8]), the associated flow rule, and power law strain-hardening. However, Barlat [2] observed that different yield functions later have been used by various researchers in the analysis of Marciniak and Kuczynski, and he found that this research shows a tremendous effect of the yield surface shape on the predicted failure limits. Furthermore, Barlat explains the reason why the failure strains are so sensitive to the yield surface shape. This explanation is shortly repeated in the following.

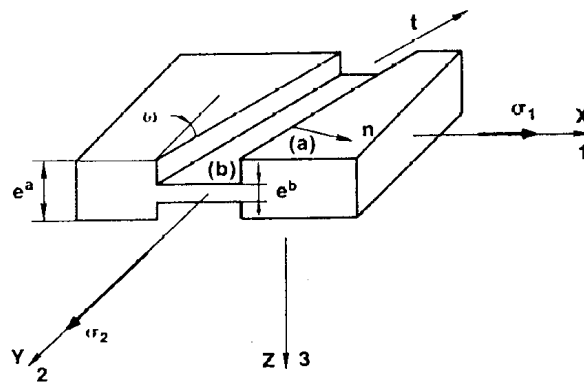


Figure 1 A drawing of the model of Marciniak and Kuczynski for localized necking (after Barlat [2]).

In the case of planar isotropy, Sowerby and Duncan [9] interpreted the process of localized necking by means of a yield locus as the one in Figure 2. Let us start considering the special case without any strain hardening. In such a case, all stress states involving plastic deformation correspond to points on the locus represented by the full line. Equilibrium requires the major principal stress to be larger inside the groove than outside it, $\sigma_{b1} > \sigma_{a1}$, during the loading process. If the loading is proportional and ignoring work hardening, the stress state in region (a) is represented by point A during the entire straining process. Since $\sigma_{b1} > \sigma_{a1}$, the stress in region (b) has to be represented by a point further along the σ_1 -axis. Assume that it is represented by point B_1 . As the strain increases, the relative thickness of the groove decreases. The major principal stress in the groove will then have to increase, and point B_1 will have to move further on along the σ_1 -axis until it reaches the limiting point B_0 . As soon as point B_1 reaches B_0 failure will occur. It is seen from Figure 2 that $\Delta\varepsilon_{b1}$ becomes large and $\Delta\varepsilon_{b2} \rightarrow 0$ as point B_1 approaches B_0 . From the assumption of plastic incompressibility it is known that $\Delta\varepsilon_{b1} + \Delta\varepsilon_{b2} + \Delta\varepsilon_{b3} = 0$, where $\Delta\varepsilon_{b3}$ is the strain increment in the thickness direction in the groove. In conclusion, $\Delta\varepsilon_{b3} = -\Delta\varepsilon_{b1}$ attains large negative values, i.e. the thickness rapidly decreases, which in reality means that the material will fracture. Even if the material strain hardens the explanation above applies. However, the rotation of point B_1 towards B_0 will be slowed down, and the material will attain a higher limiting strain. This interpretation clearly demonstrates the tremendous importance of the shape of the yield surface. Consider for instance the difference in failure strain that would be predicted using the yield surfaces of von Mises and Tresca. In the former case, the stress in the limiting point of plane stress is approximately 13% higher than the stress at balanced biaxial stress. In the latter case, however, there is no stress reserve and localization will occur at an earlier stage.

The discussion above is valid if the critical necking band is parallel to one of the principal stress directions, i.e. for materials with planar isotropy. In the case of planar anisotropy, the localized band is not necessarily parallel to one of the principal stress directions, and it is found that the shape of the yield surface in the shear stress direction is important (Barlat [2]).

It is further concluded, based on the considerations above, that the hardening rule adopted in the constitutive model may significantly alter the failure predictions for the material. Tvergaard [10] found that kinematic hardening gave far better agreement with experimental results than the assumption of isotropic hardening. In a second paper, Marciniak et al. [11] took into account the effect of strain rate and planar anisotropy, and utilized the theory to predict the FLDs for copper, steel and an aluminum alloy. They found that good results were obtained for steel and copper, but not for the aluminum alloy.

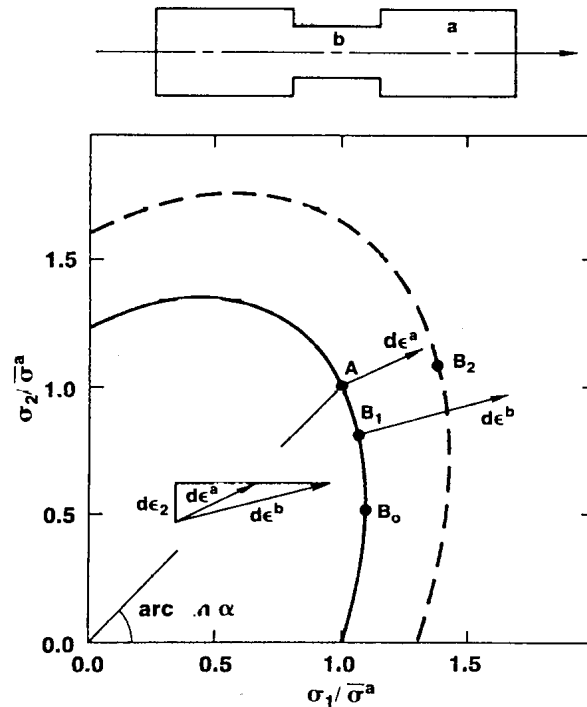


Figure 2 Interpretation of localized plastic flow (after Barlat [2]).

Thus, accurate representation of plastic instability in LS-DYNA requires proper constitutive equations and parameters for the sheet material at hand, a non-local instability criterion in the form of Eq. (2) and some inhomogeneity in geometry or material properties.

Constitutive Model

General

In the following, the equations of a constitutive model for aluminum alloys are presented. The main ingredients of the model are a yield criterion, the associated flow rule and a nonlinear isotropic hardening rule. Small strains and rotations are assumed in the presentation, while in the numerical implementation large rotations are accounted for in the co-rotational shell elements (Belytschko et al. [12]).

The strain tensor ϵ is decomposed into elastic and plastic parts (Lemaitre and Chaboche [13])

$$\epsilon = \epsilon^e + \epsilon^p \tag{3}$$

where $\boldsymbol{\varepsilon}^e$ and $\boldsymbol{\varepsilon}^p$ are the elastic and plastic strain tensors, respectively. The relation between the stress tensor $\boldsymbol{\sigma}$ and the elastic strain tensor $\boldsymbol{\varepsilon}^e$ is defined as

$$\boldsymbol{\sigma} = \mathbf{C} : \boldsymbol{\varepsilon}^e = \mathbf{C} : (\boldsymbol{\varepsilon} - \boldsymbol{\varepsilon}^p) \quad (4)$$

where \mathbf{C} is the fourth order tensor of elastic constants.

The yield function f , which defines the elastic domain in stress space, is expressed in the form

$$f = \bar{f}(\boldsymbol{\sigma}) - (\sigma_Y + R) \leq 0 \quad (5)$$

where σ_Y is the reference yield stress, R is the strain hardening variable, while the convex function \bar{f} is defined in the next section. The strain hardening is given by [13]

$$R = \sum_{i=1}^2 Q_{Ri} (1 - \exp(-C_{Ri} \bar{\varepsilon})) \quad (6)$$

where $\bar{\varepsilon}$ is the accumulated plastic strain and Q_{Ri} and C_{Ri} are strain hardening constants.

The associated flow rule defines the evolution of the plastic strain tensor and the accumulated plastic strain as [13]

$$\dot{\boldsymbol{\varepsilon}}^p = \dot{\lambda} \frac{\partial f}{\partial \boldsymbol{\sigma}}, \quad \dot{\bar{\varepsilon}} = -\dot{\lambda} \frac{\partial f}{\partial R} \quad (7)$$

where $\dot{\lambda} \geq 0$ is the plastic multiplier. The loading/unloading conditions are written in the Kuhn-Tucker form (Belytschko et al. [12])

$$f \leq 0; \quad \dot{\lambda} \geq 0; \quad \dot{\lambda} f = 0 \quad (8)$$

These equations are used to define plastic loading and elastic unloading, while the consistency condition, $\dot{f} = 0$, is utilized to determine the plastic multiplier $\dot{\lambda}$ during a plastic process.

Weak texture model (WTM)

The anisotropy observed in sheet materials is often moderate, and an acceptable accuracy may in some cases be obtained using the simple, and numerically rather efficient, yield criterion of Barlat and Lian [3]. The function \bar{f} is then defined as

$$2\bar{f}^m = a|K_1 + K_2|^m + a|K_1 - K_2|^m + c|2K_2|^m \quad (9)$$

where

$$K_1 = \frac{\sigma_x + h\sigma_y}{2} \quad (10)$$

$$K_2 = \sqrt{\left(\frac{\sigma_x - h\sigma_y}{2}\right)^2 + (p\sigma_{xy})^2} \quad (11)$$

and a , c , h , p and m are material parameters. As can be seen from the above equations, in this criterion there exists a coupling between the normal and shear stresses. Barlat [4] was the first to point out the necessity of this coupling.

Strong texture model (STM)

Extruded aluminum alloys have a severe texture, and for these materials the anisotropic yield criterion *Yld96* of Barlat and co-workers [4] is one of the best suited proposed criteria. The function \bar{f} is then defined as

$$2\bar{f}^m = \alpha_1|s_2 - s_3|^m + \alpha_2|s_3 - s_1|^m + \alpha_3|s_1 - s_2|^m \quad (12)$$

where m is a material constant, and s_1 , s_2 and s_3 are the principal values of the deviatoric, equivalent isotropic stresses \mathbf{s} , defined by the transformation $\mathbf{s} = \mathbf{L} : \boldsymbol{\sigma}$. For plane stress states and with reference axes coincident with the axes of orthotropy, the matrix representation of the tensors in the transformation is

$$\mathbf{s} = \begin{Bmatrix} s_x \\ s_y \\ s_z \\ s_{xy} \end{Bmatrix}, \quad \mathbf{L} = \frac{1}{3} \begin{bmatrix} c_2 + c_3 & -c_3 & -c_2 & 0 \\ -c_3 & c_3 + c_1 & -c_1 & 0 \\ -c_2 & -c_1 & c_1 + c_2 & 0 \\ 0 & 0 & 0 & 3c_6 \end{bmatrix}, \quad \boldsymbol{\sigma} = \begin{Bmatrix} \sigma_x \\ \sigma_y \\ \sigma_z \\ \sigma_{xy} \end{Bmatrix} \quad (13)$$

where c_1 , c_2 , c_3 and c_6 are material parameters and $\sigma_z = 0$. The principal stresses s_1 , s_2 and s_3 are determined by a procedure proposed in Yoon et al. [14]. The \mathbf{z} -axis is always a principal axis and can be assumed to coincide with the $\mathbf{3}$ -axis, so that $s_3 = s_z$. The remaining principal stresses and the angle θ between the \mathbf{x} -axis and the $\mathbf{1}$ -axis are calculated from the well-known equations

$$\begin{matrix} s_1 \\ s_2 \end{matrix} = \frac{s_x + s_y}{2} \pm \sqrt{\left(\frac{s_x - s_y}{2}\right)^2 + s_{xy}^2}, \quad \theta = \frac{1}{2} \arctan\left(\frac{2s_{xy}}{s_x - s_y}\right) \quad (14)$$

The coefficients α_1 , α_2 and α_3 are finally given as

$$\begin{aligned}\alpha_1 &= \alpha_x \cos^2 \theta + \alpha_y \sin^2 \theta \\ \alpha_2 &= \alpha_x \sin^2 \theta + \alpha_y \cos^2 \theta \\ \alpha_3 &= \alpha_{z0} \cos^2 2\theta + \alpha_{z1} \sin^2 2\theta\end{aligned}\quad (15)$$

where α_x , α_y , $\alpha_{z0} \equiv 1$ and α_{z1} are material parameters. Note, the more recent criterion Yld2000 proposed by Barlat et al. [15] has several advantages compared to Yld96 and will be utilized in future work.

Non-local Instability Criterion and the FLD Calculator

In the finite element simulations of formability with LS-DYNA, we consider a square patch of shell elements as illustrated in Figure 3, in which the element thickness varies according to a Gaussian distribution. The initial mean thickness is t_0 , while the initial width of the patch is denoted w_0 . The patch is then subjected to a set of proportional strain paths, i.e. the strain ratio, $\rho = \Delta\varepsilon_2 / \Delta\varepsilon_1$, is constant within a simulation.

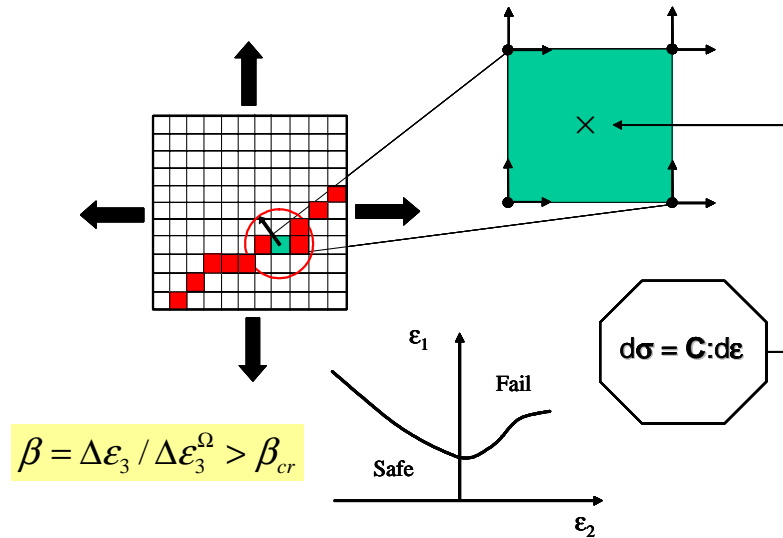


Figure 3 Concept of the non-local instability criterion and FEM-based FLD calculator

The strains are defined from

$$\varepsilon_1 = \ln \frac{w_1}{w_0}, \quad \varepsilon_2 = \ln \frac{w_2}{w_0}, \quad \varepsilon_3 = \ln \frac{t}{t_0}\quad (16)$$

where w_1 and w_2 are the current widths of the patch, and t is the current thickness. The non-local instability criterion is defined in analogy to Eq. (2). First, the increment in thickness strain $\Delta\varepsilon_3$ is calculated for all shell elements by

$$\Delta\varepsilon_3 = \frac{\Delta t}{t} \quad (17)$$

where it is recalled that the current thickness will vary from element to element due to the initial thickness variation. Second, a non-local value of the increment in thickness strain $\Delta\varepsilon_3^\Omega$ is computed for a patch of elements Ω_{el} within a user-defined radius, R_Ω , of the actual element by

$$\Delta\varepsilon_3^\Omega = \frac{1}{\Omega_{el}} \int_{\Omega_{el}} \Delta\varepsilon_3 d\Omega \quad (18)$$

The radius R_Ω is typically several times the thickness of the sheet. Third, the ratio β of the local and non-local increments in thickness strain is calculated for each shell element as

$$\beta = \frac{\Delta\varepsilon_3}{\Delta\varepsilon_3^\Omega} \quad (19)$$

Finally, localized necking is assumed to occur when $\beta \geq \beta_{cr}$ in at least one element during several consecutive time steps, where β_{cr} is a user-defined critical value of the ratio β . It is necessary for the criterion to be fulfilled during several consecutive time steps to distinguish growing instabilities from *stress waves* and *incipient, non-growing instabilities*. The critical strain state $(\varepsilon_1, \varepsilon_2)_{cr}$ is based on the global deformation of the patch at the onset of localized necking, and is computed from Eq. (16). Figure 3 illustrate the calculation of the forming limit diagram.

Validation

First the FEM-based FLD calculator is assessed by comparing the calculations with results from an analytical FLD calculator that has been implemented in Excel/Visual Basic for determination of Forming Limit Diagrams according to the Marciniak-Kuczynski analysis. The assumptions for this tool are rigid plasticity, isotropic high-exponent yield criterion, associated flow rule and non-linear isotropic hardening. It is noted that the isotropic high-exponent yield criterion is obtained from the Barlat-Lian yield criterion by taking all material constants (a , c , h , and p) equal to unity. Figure 4 compares results obtained with the classical and FEM-based FLD calculators. The material constants defining the stress-strain curve are as follows: $\sigma_0=100$ MPa, $Q=100$ MPa and $C=10$. The exponent m of the yield criterion was chosen as 2 and 8, respectively. The initial

equivalent inhomogeneity factor f_0 in the classical formability analysis was taken as 0.995, while the coefficient of variation of the thickness $CoV(t)$ in the FEM-based calculator was equal to 0.005.

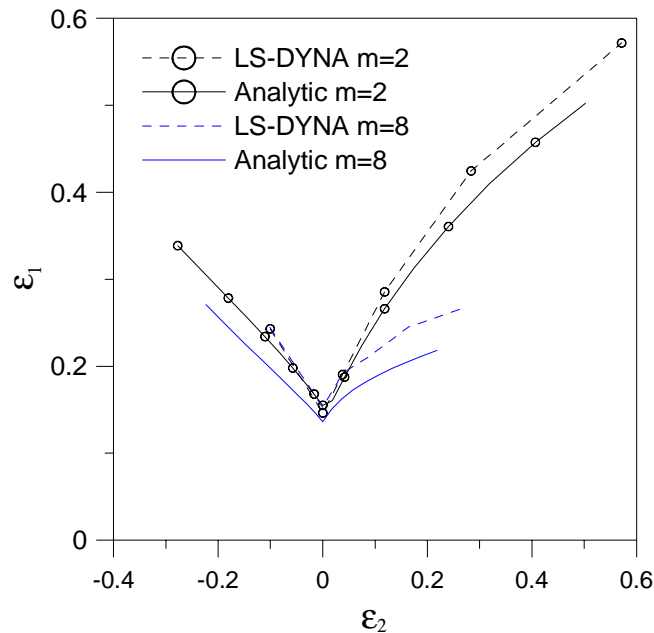


Figure 4 Effect of yield criterion exponent on FLD prediction. (Analytic: $f_0 = 0.995$. LS-DYNA: $CoV(t) = 0.005$)

There is fair agreement between the two methods when the von Mises yield criterion is adopted ($m = 2$), while the differences are more notable for the high-exponent yield criterion ($m = 8$). However, the two approaches are consistent in the sense that the strong influence of the yield surface is predicted. The advantage of the analytic approach is that it is very efficient compared to the FEM-based modeling technology, on the other hand, using FEM, physical inhomogeneity of any kind and general constitutive models can straightforwardly be represented.

Figure 5 presents experimental and numerical FLD results for a 6082 alloy in solid solution state (forming condition). The material parameters have been identified based on three uniaxial tensile tests and a through thickness compression test as explained by Barlat et al. [15] and Lademo et al. [16]. Hardening parameters used in the FEM-based calculations are given in Table 1. Anisotropy parameters for the Weak and Strong Texture Models are given in Table 2 and Table 3, respectively. The experimental formability results have been obtained using a formability test set-up similar to the one proposed by Marciniak and Kuczynski [1] measuring the strains after onset of plastic instability by use of an applied grid pattern and an automated optical measurement system. The analytic FLD calculations have been performed with an initial inhomogeneity factor of 0.995. For the FEM-based calculations 50x50 elements and a coefficient of variation of the thickness, $CoV(t)$, equal to 0.005 have been used.

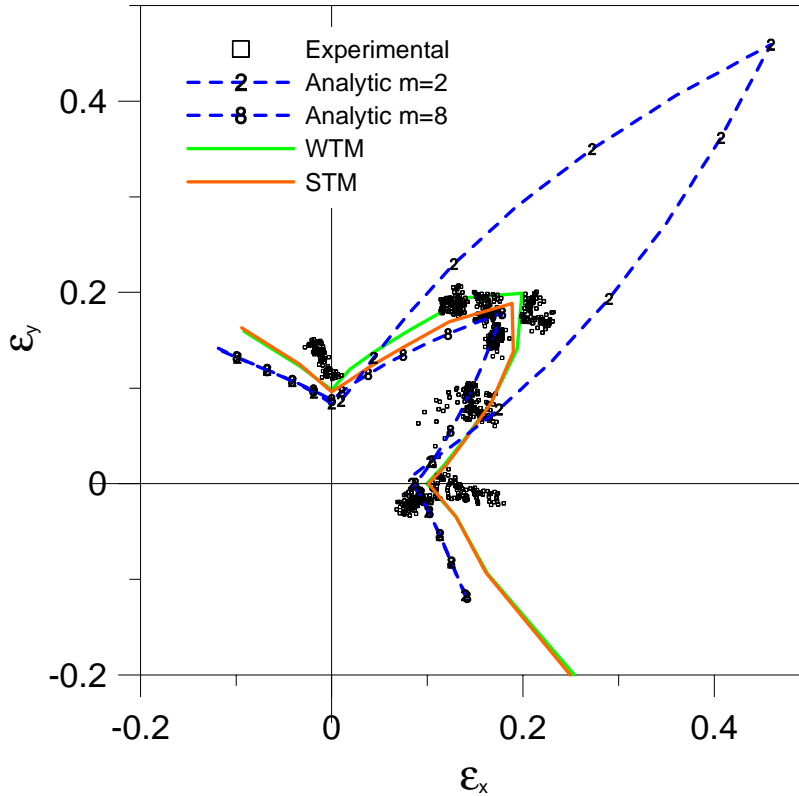


Figure 5 Experimental and predicted Forming Limit Curves AA6082-W10

Table 1 Hardening parameters for generalized Voce strain hardening rule AA6082-W10

σ_0	Q_1 [MPa]	C_1	Q_2 [MPa]	C_2
36.4	88.5	27.1	-	-

Table 2 Anisotropy parameters for AA6082-W10 – Weak Texture Model (Yld89).

a	c	h	p	m
1.115	0.885	0.980	1.160	8

Table 3 Anisotropy parameters for AA6082-W10 – Strong Texture Model (Yld96).

c_1	c_2	c_3	c_6	α_x	α_y	α_{z0}	α_{z1}	m
1.005	0.860	0.995	1.075	0.917	2.968	1.000	1.637	8

The results of the analytic FLD calculator again show that the exponent of the yield criterion plays an important role and, further, that a value of 8 gives a reasonable prediction of the FLD. An exponent equal to 2, which corresponds to the von Mises yield criterion, is seen to be very non-conservative with respect to the occurrence of plastic instability in the first quadrant of the FLD. Thus, the von Mises yield criterion should not be used in this respect for aluminum alloys. As for the isotropic case, it is seen that the formability predictions with the FEM-based FLD

calculator gives somewhat higher formability predictions than the analytic one using the chosen inhomogeneity representation.

For the chosen identification method, the formability prediction obtained using the WTM is close to the one got from the STM. If, however, biaxial stress points were obtained and that these were deviating much from the ones assumed here, the STM would probably be better at representing this additional information, and possibly the consequences with respect to formability predictions. Else, the judgment between these two models must be made with reference to the problem at hand. With respect to CPU time consumption, explicit solution of the problem is CPU intensive for both models, and a further activity should aim at using the implicit solver of LS-DYNA.

Conclusions

This paper presents how the process of loss of stability, as described by the classical analysis of Marciniak and Kuczynski, can be represented in non-linear finite element analyses with LS-DYNA. An automated procedure to calculate the formability of a material has been demonstrated. The calculations were based on two user-defined material models for weakly and strongly textured materials and a non-local instability criterion. The FEM-based formability predictions were in good agreement with experiments.

Acknowledgement

The authors gratefully acknowledge the work of Olaf Engler, Hydro Aluminium Deutschland, of acquiring the utilized uniaxial tensile test data and the importance of the European VIR* projects that funded the experiments. This work is financed through the Norlight program, supported by the Norwegian Research Council and Hydro Aluminium.

References

- [1] Z. Marciniak and K. Kuczynski, "Limit strains in the processes of stretch-forming sheet metal", *Sci.* **9** (1967), pp. 609 – 620, *Int. J. Mech. Sci.* (1967).
- [2] F. Barlat, "Crystallographic Texture, Anisotropic Yield Surfaces and Forming Limits of Sheet Metals", *Mater. Sci. Eng.*, **91** (1987), pp. 55-72.
- [3] Barlat, F., Lian, "Plastic Behaviour and Stretchability of Sheet Metals. Part I: A Yield Function for Orthotropic Sheets under Plane Stress Conditions", *International Journal of Plasticity*, **5** (1989), pp. 51-66.
- [4] F. Barlat, Y. Maeda, K. Chung, M. Yanagawa, J.C. Brem, Y. Hayashida, D.J. Lege, K. Matsui, S.J. Murtha, S. Hattori, R.C. Becker and S. Makosey, "Yield function development for aluminum alloy sheets", *J. Mech. Phys. Solids*, **45** (1997) 1727-1763.
- [5] M.G. Cockcroft and D.J. Latham, "Ductility and workability of materials", *J. Inst. Met.* **96** (1968), pp. 33–39.
- [6] Livermore Software Technology Corporation (LSTC), LS-DYNA Keyword User's Manual, Version 970, (2003)
- [7] Barata da Rocha, A., Barlat, F., Jalinier, J.M., *Materials Science and Engineering*, **68** (1984), 151.

- [8] Hill, R., "The Mathematical Theory of Plasticity", Oxford: Clarendon Press (1950).
- [9] Sowerby, R., Duncan, J.L., "Failure in Sheet Metal in Biaxial tension", *Int. J. Mech. Sci.*, **13** (1971), pp. 217-229.
- [10] Tvergaard, V., "Effect of Kinematic Hardening on Localized Necking in Biaxially Stretched Sheets", *Int. J. Mech. Sci.*, **20** (1978), pp. 651-658.
- [11] Marciniak, Z., Kuczinsky, K., Pokora, T., "Influence of the Plastic Properties of a material on the Forming Limit Diagram for Sheet Metals in Tension", *Int. J. Mech. Sci.*, **15** (1973), pp. 789-805.
- [12] T. Belytschko, W.K. Liu and M. Moran, "Nonlinear Finite Elements for Continua and Structures", Wiley, 2000.
- [13] J. Lemaitre and J.-L. Chaboche, "Mechanics of Solid Materials", Cambridge University Press, 1990.
- [14] J.W. Yoon, F. Barlat, K. Chung, F. Pourboghhrat, and D.Y. Yang, "Influence of initial back stress on the earing prediction of drawn cups for planar anisotropic aluminium sheets", *J. Mater. Proc. Tech.* **80-81** (1998) 433-437.
- [15] F. Barlat, J.C. Brem, J.W. Yoon, K. Chung, R.E. Dick, D.J. Lege, F. Poruboghhrat, S.-H. Choi, E. Chu, "Plane stress yield function for aluminium alloy sheets – Part 1: theory", *International Journal of Plasticity*, **19** (2003), pp. 1297-1319.
- [16] O.-G. Lademo, K.O. Pedersen, T. Berstad and O.S. Hopperstad "Validation of a formability prediction tool for aluminium alloys", To be presented at the Metal Forming 2004, Krakow, Poland.